Geological Magazine

www.cambridge.org/geo

Rapid Communication

Cite this article: Esteban JJ, Cuevas J, Tubía JM, Hilario A, Larionov A, and Sergeev S (2021) Posets pluton: a geochronological piece in the puzzle of the Axial Zone of the Pyrenees. *Geological Magazine* **158**: 2264–2270. https://doi.org/10.1017/S0016756821000686

Received: 10 December 2020
Revised: 14 June 2021
Accepted: 17 June 2021
First published online: 10 August 2021

Keywords:
Pyrenees; Axial Zone; Posets pluton; U–Pb SHRIMP; LA-ICP-MS

Author for correspondence: JJ Esteban, Email: jj.esteban@ehu.es

CAMBRIDGE UNIVERSITY PRESS

Posets pluton: a geochronological piece in the puzzle of the Axial Zone of the Pyrenees

JJ Esteban[1], J Cuevas[1], JM Tubía[1], A Hilario[2], A Larionov[3] and S Sergeev[3]

[1]Departamento de Geología, Facultad de Ciencia y Tecnología, Universidad del País Vasco UPV/EHU, apartado 644, 48080 Bilbao, Spain; [2]Basque Coast UNESCO Global Geopark, Ifar Kalea 4, 20820 Deba, Spain and [3]Centre of Isotopic Research, VSEGEI, 199106 St Petersburg, Russia

Abstract

A detailed geochronological study was conducted on zircons from a diorite sample of the Posets pluton (Axial Zone, Pyrenees). The extracted igneous zircons constrain the emplacement of the pluton to 302 ± 2 Ma and 301 ± 3 Ma, by means of U–Pb sensitive high-resolution ion microprobe (SHRIMP) and laser ablation inductively coupled plasma mass spectrometry (LA-ICP-MS) analyses, respectively. Considering the syn- to late-tectonic emplacement of the Posets pluton during the main Variscan deformation event (D_2), the obtained ages constrain the long-lasting D_2, associated with the dextral transpression registered through the Axial Zone of the Pyrenees.

1. Introduction

The Pyrenees, the E–W-trending orogenic belt that runs parallel to the French–Spanish border, were raised in response to the convergence of the Iberian and European plates in Cenozoic times. A main feature of this belt is its asymmetric fan shape with opposed vergences of the principal Alpine structures that rework previous Variscan ones. The North and South Pyrenean Zones, where sedimentary rocks of Mesozoic and Cenozoic ages predominate, border the Axial Zone of the Pyrenees. The Pyrenean Axial Zone is a fragment of the European Variscan belt incorporated into the core of the Pyrenean mountain range from Cretaceous to Miocene times (Mattauer, 1968; Matte, 1991). The rocks that currently make up the Axial Zone experienced a complex Variscan tectonothermal evolution resulting from overall compressional tectonics dominated by dextral transpression (e.g. Bouchez & Gleizes, 1995; Gleizes *et al.* 1998*a*; Carreras & Druguet, 2014). The main Variscan tectonic phase, D_2 (Gleizes *et al.* 1998*a*), corresponds to a transpressional event characterized by N120° E-directed great hectometric tight folds verging southwest. A penetrative foliation (S_2) develops parallel to the axial plane of these folds, temporally close to the thermal peak of the metamorphism (Gleizes *et al.* 1998*b*). Late tectonic phases generated localized strike-slip ductile shear zones in granitoids and high-grade metamorphic rocks (Carreras & Capellà, 1994). In this context, the Variscan magmatism in the Pyrenees is mainly represented by calc-alcaline plutons of granite to granodiorite compositions emplaced into intermediate to shallow structural levels.

Structural and anisotropy-of-magnetic-susceptibility (AMS) studies of the granitoids in the Pyrenees (Porquet *et al.* 2017) have demonstrated that their emplacement was coeval with the main Variscan D_2 transpressive event (see Bouchez & Gleizes, 1995; Carreras & Druguet, 2014). Most plutons are of Carboniferous age and their emplacement age extends over 70 Myr from 339–337 Ma (granite stocks situated in the core of the Ordovician Aston and Bossòst domes; Mezger & Gerdes, 2016) to 267 ± 1 Ma (Aya pluton in the Western Pyrenees; Denèle *et al.* 2012). This long timespan makes it difficult to establish an accurate time relationship between the development of S_2 and the emplacement age for any given pluton from geological constraints alone.

In this work, we present new U–Pb sensitive high-resolution ion microprobe (SHRIMP) and laser ablation inductively coupled plasma mass spectrometry (LA-ICP-MS) analyses of zircons from a diorite sample of the Posets pluton (PO-52) to determine the precise age for the emplacement of the pluton.

2. Geological setting

The Posets pluton has a slightly elliptical shape on a map, with an aspect ratio (short to long axis quotient) of 0.85 and a N130° E elongation (Fig. 1). From the petrographic point of view, it displays a normal and concentric compositional zoning (Fig. 2), with a gradual transition ranging from granodiorite in the inner part to tonalite towards peripheral zones (Enrique, 1989; A Hilario, unpub. PhD thesis, Univ. Basque Country, 2004). Diorite is locally found in the border tonalite zone. All of these facies have a very homogeneous fine-grained holocrystalline

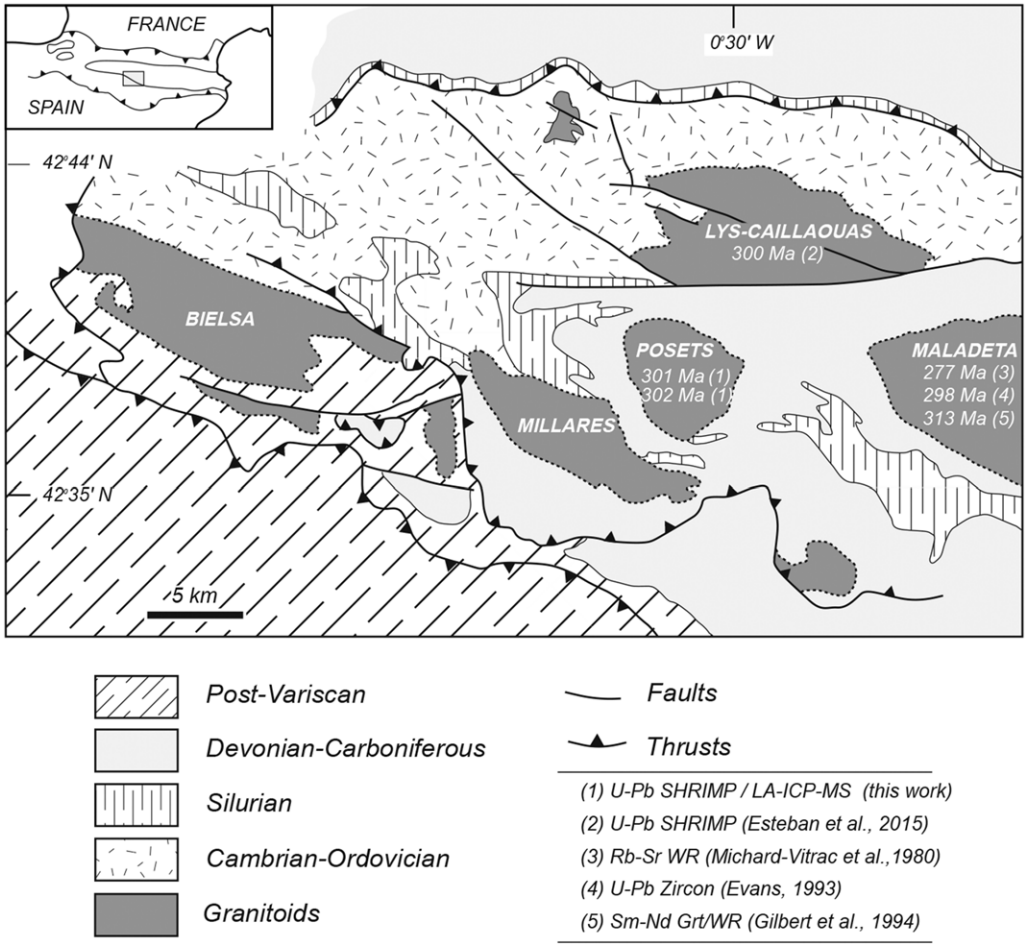

Fig. 1. Schematic geological map of the Central Pyrenees with the Posets pluton location (modified from Vissers, 1992).

(*c.* 2–3 mm) texture and include microgranular enclaves with angular borders and xenoliths from the country rocks that preserve S_2, and even S_2-related folds occasionally. The dominant mineralogical composition in the Posets pluton consists of quartz, plagioclase, K-feldspar, biotite, amphibole and sphene. Geochemical data from 12 igneous samples reflect calc-alkaline and alumino-cafemic trends and point to a hybrid magmatic source for the Posets pluton (A Hilario, unpub. PhD thesis, Univ. Basque Country, 2004). *P–T* estimations of two samples from the Posets pluton using the 'amphibole–plagioclase' geothermometer (Blundy & Holland, 1990) and 'Al-in-hornblende' geobarometer (Schmidt, 1992) yielded temperatures and pressures of 719 ± 30 °C / 1.9 ± 0.2 kbar and 728 ± 20 °C / 1.6 ± 0.2 kbar, respectively (A Hilario, unpub. PhD thesis, Univ. Basque Country, 2004).

The Posets granite intrudes into slates and limestones of Silurian to Lower–Medium Devonian age (Figs 1 and 2). The contact with the country rocks is sharp and generally concordant with the bedding and the main tectonic foliation (S_2) of the country rocks. This foliation is an axial-planar cleavage associated with isoclinal upright folds next to the northern pluton contact and tight, south-verging folds in the southern contact zone. These structures form part of a progressive process of coaxial deformation that led to fold interference patterns of type 3. As the dominant foliation is linked to the youngest folding stage, it is referred to as S_2. There is a previous cleavage (S_1) that can be recognized in the field, crenulated by S_2 in hinges of D_2-folds. The preservation of S_1 is fairly widespread at the thin-section scale, as a residual foliation crenulated by S_2 in intrafoliar folds in samples from the limbs of young folds. At the regional scale, the strike of S_2 ranges between N90° and N120° E, with an average dip of 50° N (Fig. 2). The trajectories of the S_2 cleavage are, however, distorted at the eastern and western edges of the Posets pluton, where foliation triple points developed (Fig. 2). The country rocks were affected by a weak regional metamorphism that reached green-schist facies conditions. The pluton intrusion also produced a metamorphic aureole of 1 km thickness (Fig. 2), represented by andalusite/cordierite-bearing or even sillimanite-bearing hornfels very near the intrusive contact and mineral associations with garnet ± diopside ± epidote and minor olivine in the marbles (A Hilario, unpub. PhD thesis, Univ. Basque Country, 2004). In most areas of the metamorphic aureole these minerals grow on S_2 as idiomorphic porphyroblasts with random orientations, but they appear as porphyroclasts with pressure shadows in a narrow fringe (nearly 10 m thick) on the innermost southern aureole. This solid-state deformation has its counterpart in sparse dextral S-C mylonites developed in tonalites that are in contact with the country rocks.

Field and AMS data from the Posets pluton (García Maiztegi *et al.* 1991; A Hilario, unpub. PhD thesis, Univ. Basque Country, 2004) reveal a concentric structural pattern, defined by spatial variations in the orientation of the magmatic and magnetic foliations (Fig. 2). The internal structure is roughly parallel to the pluton border. The foliation trajectories display a NW–SE ellipsoidal geometry with variable NNE dips, moderate dips and steep dips dominating in the southern and northern part of the pluton,

https://doi.org/10.1017/S0016756821000686 Published online by Cambridge University Press

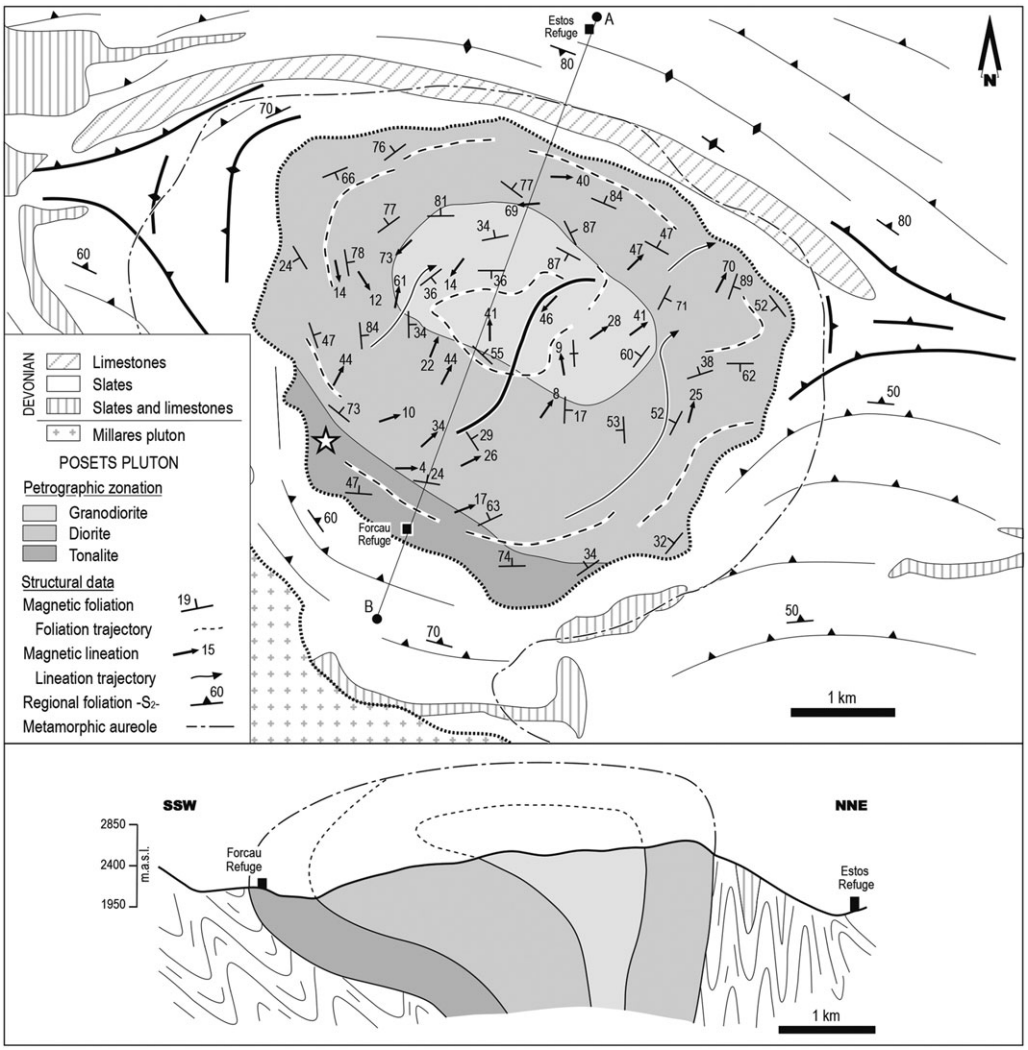

Fig. 2. Structural map (modified from A Hilario, unpub. PhD thesis, Univ. Basque Country, 2004) and synthetic cross-section (A–B) of Posets pluton. The star indicates the analysed sample location. Foliation data of the country rocks were also compiled from Ríos *et al.* (1982, 2002).

respectively (Fig. 2). In contrast, the N- and NE-plunging magnetic lineation outlines S-shaped sigmoidal patterns (A Hilario, unpub. PhD thesis, Univ. Basque Country, 2004).

3. U–Pb SIMS SHRIMP dating

A diorite sample (PO-52: 42° 38′ 3.52″ N, 0° 27′ 8.52″ E) was processed according to routine zircon mineral separation (crushing, grinding, sieving under 250 μm, Wilfley table, Frantz isodynamic magnetic separator and methylene iodide) at the University of the Basque Country (UPV/EHU). The selected zircon crystals were placed in epoxy resin together with the TEMORA 1 and 91500 reference zircons, sectioned approximately in half, polished and analysed on a SHRIMP-II SIMS at the Centre of Isotopic Research (CIR) at VSEGEI (St Petersburg). The results were obtained following the procedure described by Larionov *et al.* (2004). The U–Pb ion microprobe data were processed with the SQUID 1.02 (Ludwig, 2001) and Isoplot/Ex 3.00 (Ludwig, 2003) software using the decay constants of Steiger and Jäger (1977) and are presented in Appendix Table 1 (in the Supplementary Material available online at https://doi.org/10.1017/S0016756821000686). Cathodoluminescence images were used to select target areas for analysis.

Most of the analysed zircon crystals are devoid of inherited cores and present: (1) prismatic and euhedral morphologies, (2) concentric undisturbed oscillatory growth zoning (both in Fig. 3) and (3) high Th/U ratios, scattered between 0.42 and 0.76 (Fig. 4). The few composite zircons that display inherited xenomorphic cores (e.g. zircon crystals 3.1 and 10.1 in Fig. 3) are surrounded by an external rim with concentric oscillatory zoning. These cores display corroded and rounded geometries, oscillatory zoning and high Th/U ratios (0.87). Ten local analyses were carried out (online Appendix Table 1, in the Supplementary Material available online at https://doi.org/10.1017/S0016756821000686) in the oscillatory zoned parts of single zircons and in the external parts of composite zircon crystals (zircon crystals 3.1 in Fig. 3). These analyses yielded a ^{238}U–^{206}Pb Concordia age of 302 ± 2 (2σ) Ma (Fig. 5). Otherwise, the spot analyses taken from a xenomorphic and rounded core afford a Neoarchaean age (online Appendix Table 1, in the Supplementary Material available online at https://doi.org/10.1017/S0016756821000686).

4. U–Pb LA-ICP-MS dating

Zircon crystals were analysed by LA-ICP-MS at the University of the Basque Country (SGIker) using a 213 nm New Wave Nd:YAG laser with a pulse energy density of ~4 J cm^{-2} and a frequency of 10 Hz coupled to a Thermo Fisher XSeries-2 quadrupole ICP-MS. The analytical spot size was 40 μm in diameter, and in most cases

https://doi.org/10.1017/S0016756821000686 Published online by Cambridge University Press

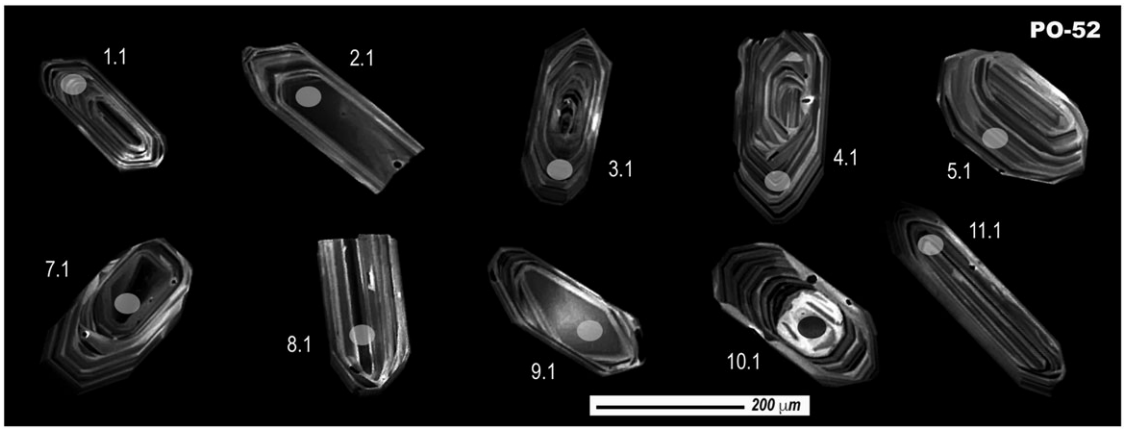

Fig. 3. Cathodoluminescence images of analysed zircon crystals by SHRIMP.

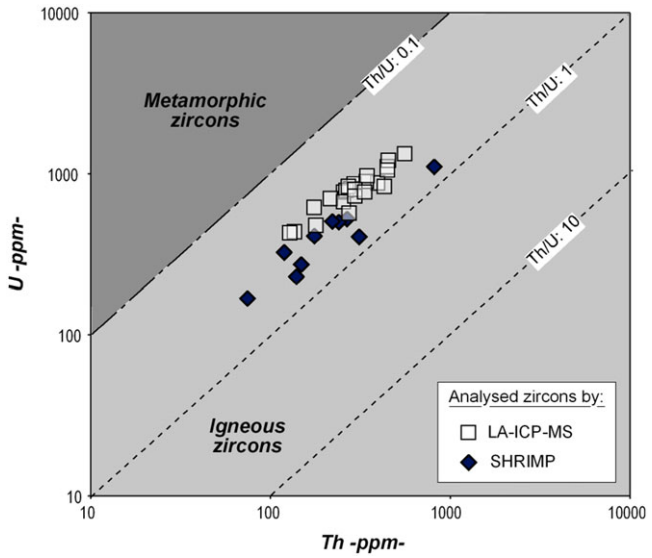

Fig. 4. Discriminatory and compositional U vs Th diagram of the analysed zircon crystals

the zircon crystals were completely pierced through. Analytical acquisition times were up to 56 s. The external calibration was performed to GJ-1 zircon, and the laboratory staff reduced the data using the Iolite 2.5 software package (Paton *et al.* 2011; Paul *et al.* 2012).

Following the acquisition of the electron backscattered images with a JEOL 6400-JSM of the University of the Basque Country (UPV/EHU-SGIker), only the prismatic zircon crystals with oscillatory zoning (Fig. 6) were selected as targets. These prismatic zircons also have high Th/U ratios (0.28–0.50; Appendix Table 2, in the Supplementary Material available online at https://doi.org/10.1017/S0016756821000686; Fig. 4). Thirty zircon crystals were analysed and seven of them were rejected, due to their discordant ages, for the geological interpretation (online Appendix Table 2, in the Supplementary Material available online at https://doi.org/10.1017/S0016756821000686). Data from the analysed spots were projected on a $^{207}Pb/^{206}Pb$ vs $^{238}U/^{206}Pb$ diagram (Tera & Wasserburg, 1972). Twenty-three of the 30 analyses (online Appendix Table 2, in the Supplementary Material available online at https://doi.org/10.1017/S0016756821000686) yielded a lower interception age of 302 ± 3 (2σ) Ma (Fig. 7). The weighted average $^{206}Pb–^{238}U$ age of 301 ± 3 (2σ) Ma (Fig. 7) also agrees with the result obtained by means of U–Pb SHRIMP analysis.

5. Discussion

The 3-D geometry of the Posets pluton is well constrained as an asymmetric inverted drop tilted towards the south (A Hilario, unpub. PhD thesis, Univ. Basque Country, 2004), which is also consistent with the southward vergence of the major Variscan folds and the N-dipping associated slate cleavage, S_2, in the country rocks (Fig. 2). The pressure crystallization conditions specified for the Posets pluton suggest an emplacement level at depths of *c.* 4 km (A Hilario, unpub. PhD thesis, Univ. Basque Country, 2004). An issue that requires further clarification is the temporal relationships between the emplacement and the development of the metamorphic aureole at this shallow level with the inclusion of metamorphic roof-pendants that preserve the S_2 and S_1 cleavages. Gleizes *et al.* (1998*b*) reported similar observations in the country rocks of the Cauterets–Panticosa pluton. This observation would apparently conflict with a synkinematic emplacement during D_2 and could be interpreted as evidence of a postkinematic emplacement. However, the following structural and regional arguments seem to support its emplacement during an event of dextral transpression associated with D_2: (1) the Posets pluton is confined between two other granites (Fig. 1), 2 km to the SW of the Lys pluton (Hilario *et al.* 2003) and 1 km to the NE of the Millares pluton (Román-Berdiel *et al.* 2006), the emplacement of which took place under dextral transpression at the end of D_2; (2) the emplacement ages of the Posets (this work) and Lys (Esteban *et al.* 2015) plutons agree within the error limits; and (3) the existence of S-shaped lineation patterns in the Posets pluton is similar, in both its layout and orientation (Fig. 2), to sigmoidal lineation patterns that have been linked with dextral transpression in many other synkinematic Pyrenean granites (Bouchez & Gleizes, 1995; Gleizes *et al.* 1998*b*; Román-Berdiel *et al.* 2004; Porquet *et al.* 2017). It thus seems reasonable to consider the Posets pluton as a syn- to late-kinematic granite emplaced during the dextral transpression triggered at the end of the long-lasting Variscan deformational event (D_2). Therefore, the foliation in the roof-pendants and xenoliths would correspond to incipient stages in the development of the S_2 foliation within the framework of a long-lasting regional stress field, whereas the pluton

https://doi.org/10.1017/S0016756821000686 Published online by Cambridge University Press

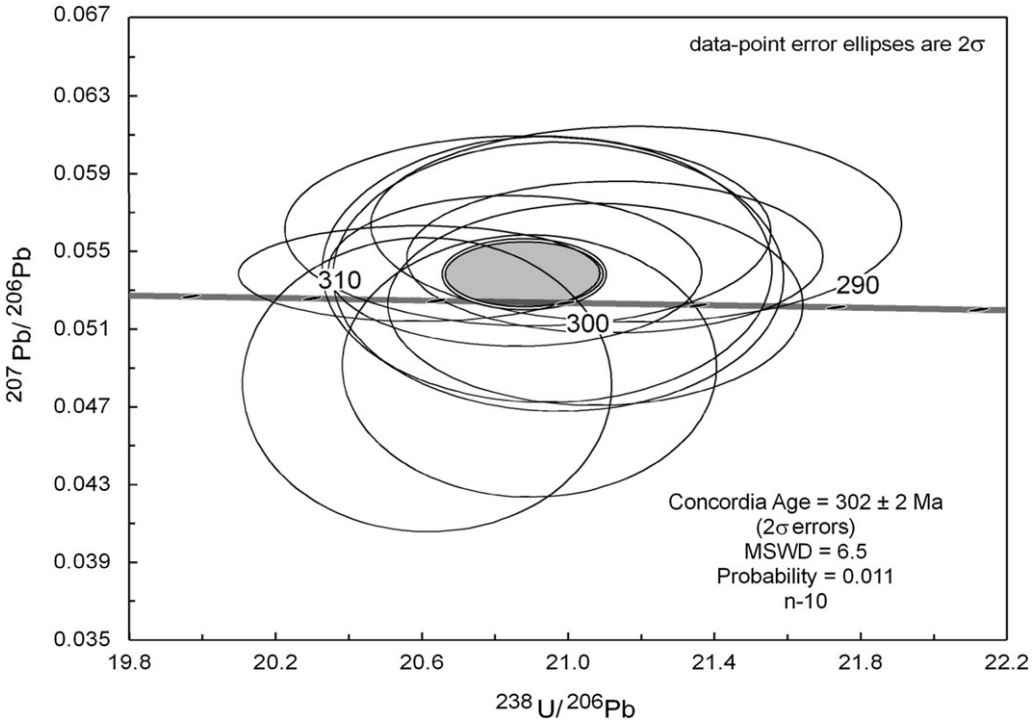

Fig. 5. Tera–Wasserburg plot of the analysed zircon crystals by SHRIMP.

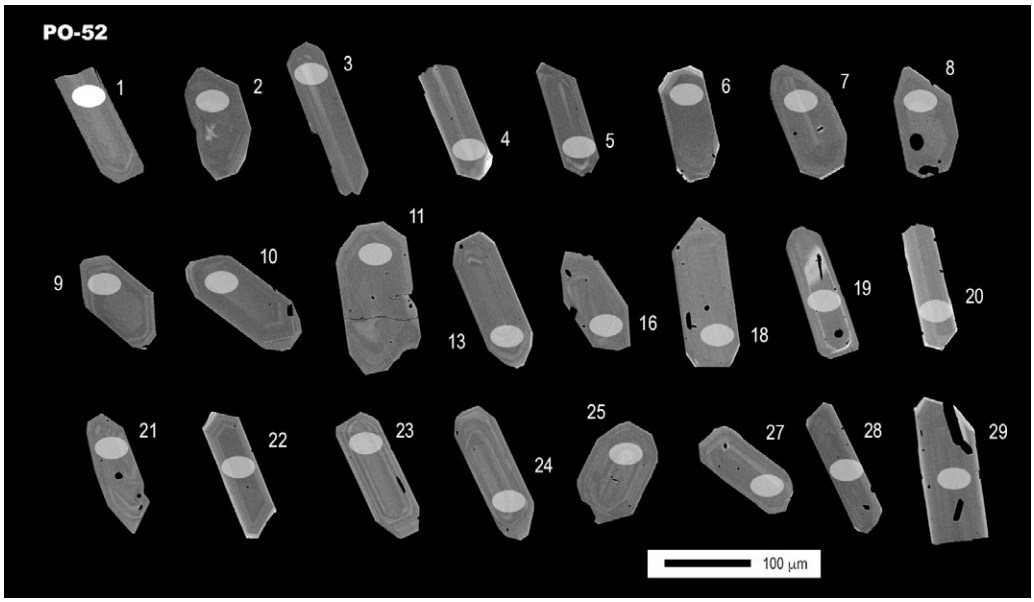

Fig. 6. Backscattered electron images of zircon crystals analysed by LA-ICP-MS.

emplacement and the development of the metamorphic aureole are short-lived processes that took place in a subsequent stage.

Our new geochronological data (U–Pb SHRIMP and LA-ICP-MS zircon analyses) from the Posets pluton provide a fairly accurate age of 302 ± 2 Ma. Considering that the morphological features and high Th/U ratios (>0.1; e.g. Hoskin & Schaltegger, 2003) of the zircon crystals are consistent with its magmatic origin, the result obtained (≈302 Ma) can be considered as the emplacement age of the Posets pluton. The emplacement age of most syn-kinematic plutons (syn-D_2) from the central Pyreneees falls into a broad timespan constrained between 298 and 310 Ma: for example: 301 ± 9 Ma for the Eaux-Chaudes massif (Guerrot, 2001; Ternet *et al.* 2004); 301 ± 9 Ma (Guerrot, 1998) and 306 ± 2 Ma (Denèle *et al.* 2014) in the Eastern Cauterets pluton; 298 ± 2 Ma (NG Evans, unpub. PhD thesis, Univ. Leeds, 1993) and 303 ± 4 Ma (Pereira *et al.* 2014) in the Maladeta massif; 309 ± 4 Ma (Gleizes *et al.* 2006) for the Bordères–Louron pluton; and 300 ± 2 Ma (Esteban *et al.* 2015) for the Lys pluton. The new age, 302 ± 2 Ma, we have obtained for the emplacement of the Posets pluton fits into the time range specified for the emplacement of the above-mentioned syn-D_2 granite plutons of the central Pyrenees (298 to 310 Ma).

A few Pyrenean granite plutons have yielded much younger ages: 267.1 ± 1.1 Ma in the Aya pluton (Denèle *et al.* 2012) and 279.6 ± 3 Ma in the Vielha granodiorite (Pereira *et al.*, 2014), for example. These ages nearly overlap with those of the Permian

https://doi.org/10.1017/S0016756821000686 Published online by Cambridge University Press

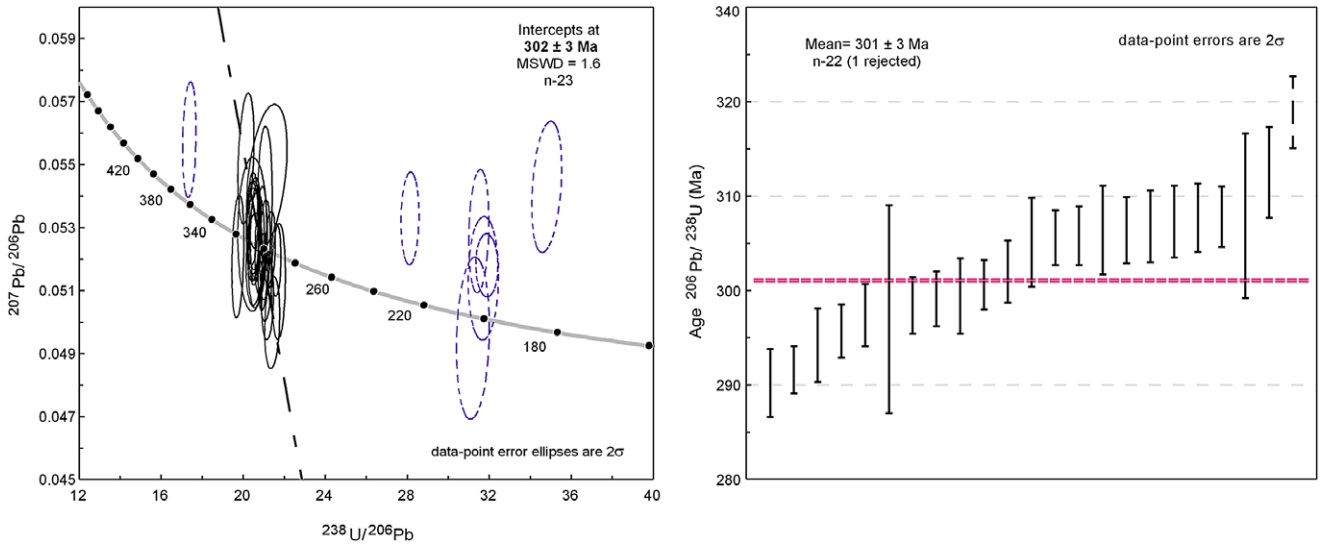

Fig. 7. (Colour online) Tera–Wasserburg plot and weighted average U–Pb age of the analysed zircon crystals by LA-ICP-MS.

volcanism recognized more than 60 km to the west, in the Midi d'Ossau and Anayet volcanic edifices (278–272 Ma; Briqueu & Innocent, 1993) or in subvolcanic dykes from the Sallent area (259 ± 3.2 Ma; Rodríguez-Méndez *et al.* 2014). Owing to this time convergence, it has been suggested that the Aya pluton would mark the transition from the late Variscan transpression to dextral transtensional conditions that first promoted the opening of Stephanian–Permian basins and subsequently led to the formation of the Bay of Biscay rift during the Mesozoic extension (Dènele *et al.* 2012). In contrast, according to Pereira *et al.* (2014), the magmatism of the Variscan Pyrenean would be the expression of the subduction of the Palaeotethys Ocean in a long time interval, from *c.* 304 Ma to *c.* 266 Ma. Nevertheless, certain regional issues would question the geological meaning of the youngest ages of the Pyrenean granites. For instance, according to Pesquera and Pons (1990) and Olivier *et al.* (1999) the Aya Pluton was synkinematically emplaced during the main D_2 tectonic phase that is unconformably sealed by Stephanian deposits (Campos, 1979). If true, these facts would require an emplacement older than 290 Ma for the Aya pluton and the age of 267.1 ± 1.1 Ma (Denèle *et al.* 2012) could reflect the younging effect of the Alpine Aritxulegi fault that completely traverses the pluton. Regarding the Vielha granodiorite the sample is very close to the southern contact of the pluton (Pereira *et al.* 2014; Fig. 2), which could have been reactivated as a shear zone during the Alpine orogeny (Leblanc *et al.* 1994). Consequently, further geochronological work focused on the possible overprinting effect of the Alpine orogeny would be desirable to test these interpretations.

6. Conclusions

(1) U–Pb SHRIMP and LA-ICP-MS analysis of zircon crystals from a diorite of the Posets pluton yields an age ~302 Ma for its emplacement in the Variscan upper crust, now the Axial Zone of the Pyrenees, in shallow depth conditions.

(2) The obtained age fits into the wide timespan (310 to 298 Ma) established from other synkinematic plutons of the central Pyrenees.

(3) The emplacement and development of the metamorphic aureole must be considered as short-lived events along the long-lasting D_2 deformational process that led to S_2 formation in a dextral transpressional field.

Supplementary material. To view supplementary material for this article, please visit https://doi.org/10.1017/S0016756821000686

Acknowledgements. This work was supported by grants EHUA13/03 and GIU20/017 from the University of the Basque Country (UPV/EHU) and CGL2017-82976 from the Ministerio de Economía, Industria y Competitividad / Agencia Estatal de Investigación / Fondo Europeo de Desarrollo Regional, European Union. E. Druguet, Y. Denèle, an anonymous reviewer and the editor Olivier Lacombe are thanked for reviews and discussions that improved the final manuscript.

Declaration of Interest. There are no potential conflicts of interest.

References

Blundy JD and Holland TJB (1990) Calcic amphibole equilibria and new amphibole-plagioclase geothermometer. *Contributions to Mineralogy and Petrology* **104**, 208–24. doi: 10.1007/BF00306444.

Bouchez JL and Gleizes G (1995) Two-stage deformation of the Mont-Louis-Andorra granite pluton (Variscan, Pyrenees) inferred from magnetic susceptibility anisotropy. *Journal of the Geological Society, London* **152**, 669–79. doi: 10.1144/gsjgs.152.4.0669.

Briqueu L and Innocent C (1993) Datation U/Pb sur zircon et géochimie isotopique Sr et Nd du volcanisque permien des Pyrénées occidentales (Ossau et Anayet). *Comptes Rendus de l'Académie des Sciences, Paris* **316**, 623–8.

Campos J (1979) Estudio geológico del Pirineo vasco al W del río Bidasoa. *Munibe* **1–2**, 3–139.

Carreras J and Capellà I (1994) Tectonic levels in the Paleozoic basement of the Pyrenees: a review and a new interpretation. *Journal of Structural Geology* **16**, 1509–24. doi: 10.1016/0191-8141(95)00049-J.

Carreras J and Druguet E (2014) Framing the tectonic regime of the NE Iberian Variscan segment. In *The Variscan Orogeny: Extent, Time Scale, and the Formation of the European Crust* (eds K Schulmann, JR Martínez Catalán, JM Lardeaux, V Janousek and G Oggiano), pp. 249–64. Geological Society of London, Special Publication no. 405. doi: 10.1144/SP405.7.

Denèle Y, Laumonier B, Paquette J-L, Olivier P, Gleizes G and Barbey P (2014) Timing of granite emplacement, crustal flow and gneiss dome formation in the

Variscan segment of the Pyrenees. In *The Variscan Orogeny: Extent, Timescale and Formation of the European Crust* (eds K Schulmann, JR Martínez Catalán, JM Lardeaux, V Janousek and G Oggiano), pp. 265–7. Geological Society of London, Special Publication no. 405. doi: 10.1144/SP405.5.

Denèle Y, Paquette J-L, Olivier P and Barbey P (2012) Permian granites in the Pyrenees: the Aya pluton (Basque Country). *Terranova* **24**, 105–13. doi: 10.1111/j.1365-3121.2011.01043.x.

Enrique P (1989) Caracterización geoquímica mediante elementos mayores de los granitoides de la vertiente meridional del Pirineo Central. *Studia Geologica Salmanticensia* **4**, 41–60.

Esteban JJ, Aranguren I, Cuevas J, Hilario A, Tubía JM, Larionov A and Sergeev S (2015) Is there a time lag between the metamorphism and emplacement of plutons in the Axial Zone of the Pyrenees? *Geological Magazine* **152**, 935–41. doi: 10.1017/S001675681500014X.

García Maiztegi, Aranguren A and Tubía JM (1991) Zonación magnética y caracterización del elipsoide de la susceptibilidad magnética en el plutón de Posets (Pirineos Centrales). *Geogaceta* **10**, 38–40.

Gilbert JS, Bickle MJ and Chapman HJ (1994) The origin of Pyrenean Hercynian volcanic rocks (France-Spain): REE and Sm-Nd isotope constraints. *Chemical Geology* **111**, 207–26. doi: 10.1016/0009-2541(94)900090-6.

Gleizes G, Crevon G, Asrat A and Barbey P (2006) Structure, age and mode of emplacement of the Hercynian Bordères-Louron pluton (Central Pyrenees, France). *International Journal of Earth Sciences* **95**, 1039–52. doi: 10.1007/s00531-006-0088-4.

Gleizes G, Leblanc D and Bouchez JL (1998a) The main phase of the Hercynian orogeny in the Pyrenees is a dextral transpression. In *Continental Transpressional and Transtensional Tectonics* (eds RE Holdsworth, RA Strachan and JF Dewey), pp. 267–73. Geological Society of London, Special Publication no. 135. doi: 10.1144/GSL.SP.1998.135.01.17.

Gleizes G, Leblanc D, Santana V, Olivier P and Bouchez JL (1998b) Sigmoidal structures featuring dextral shear during emplacement of the Hercynian granite complex of Cauterets-Panticosa (Pyrenees). *Journal of Structural Geology* **20**, 1229–45. doi: 10.1016/S0191-8141(98)00060-1.

Guerrot C (1998) Résultats de datation U-Pb par dissolution sur zircons pour le granite de Cauterets, Pyrénées. Rapport inédit, SMN/PEA/ISO 146/98 CG/NB, BRGM. In *Notice explicative, Carte géologique de la France (1/50000), feuille Gabarnie (1082)* (eds C Majesté-Menjoulas, F Debon and P Barrère), p. 4. Orléans: BRGM.

Guerrot C (2001) Datation du pluton des Eaux-Chaudes. In *Notice explicative, Carte géologique de la France (1/50000), feuille Laruns-Somport (1069)* (eds Y Ternet, C Majesté-Menjoulas, J Canérot, T Baudin, A Cocherie, C Guerrot and P Rossi), pp. 185–7. Orléans: BRGM.

Hilario A, Aranguren A, Tubía JM and Pinotti L (2003) Estructura del Plutón sincinemático de Lys (Zona Axial del Pirineo). *Geogaceta* **34**, 51–4.

Hoskin PWO and Schaltegger U (2003) The composition of zircon and igneous and metamorphic petrogenesis. *Reviews in Mineralogy and Geochemistry* **53**, 25–104. doi: 10.2113/0530027.

Larionov AN, Andreichev VA and Gee DG (2004) The Vendian alkaline igneous suite of the northern Timan: ion microprobe U-Pb zircon ages of gabbros and syenite.. In *The Neoproterozoic Timanide Orogen of Eastern Baltica* (eds DG Gee and VL Pease), pp. 69–74. Geological Society of London, Memoirs 30. doi: 10.1144/GSL.MEM.2004.030.01.07.

Leblanc D, Gleizes G, Lespinasse P, Olivier Ph and Bouchez JL (1994) The Maladeta granite polydiapir, Spanish Pyrenees: a detailed magneto-structural study. *Journal of Structural Geology* **16**, 223–35. doi: 10.1016/0191-8141(94)90106-6.

Ludwig KR (2001) *SQUID 1.02: A User's Manual, A Geochronological for Microsoft Excel*. Berkeley, California: Berkeley Geochronology Center Special Publication.

Ludwig KR (2003) *User's Manual for Isoplot/Ex, Version 3.00, A Geochronological Toolkit for Microsoft Excel*. Berkeley, California: Berkeley Geochronology Center Special Publication.

Mattauer M (1968) Les traîts structuraux essentiels de la Chaîne pyrénéenne. *Revue de Géographie Physique et de Géologie Dynamique* **10**, 3–12.

Matte P (1991) Accretionary history and crustal evolution of the Variscan belt in Western Europe. *Tectonophysics* **196**, 309–27. doi: 10.1016/0040-1951(91)90328-P.

Mezger JE and Gerdes A (2016) Early Variscan (Visean) granites in the core of central Pyrenean gneiss domes: implications from laser ablation U-Pb and Th-Pb studies. *Gondwana Research* **29**, 181–98. doi: 10.1016/j.gr.2014.11.010.

Michard-Vitrac A, Albarede F, Dupuis C and Taylor HP Jr (1980) The genesis of Variscan (Hercynian) plutonic rocks: inferences from Sr, Pb and O studies of the Maladeta Igneous Complex, Central Pyrenees (Spain). *Contributions to Mineralogy and Petrology* **72**, 57–72.

Olivier P, Améglio L, Richen H and Vadeboin F (1999) Emplacement of the Aya Variscan pluton (Basque Pyrenees) in a dextral transcurrent regime inferred from a combined magneto-structural and gravimetric study. *Journal of the Geological Society, London* **156**, 991–1002.

Paton C, Hellstrom J, Paul B, Woodhead J and Hergt J (2011) Iolite: freeware for the visualisation and processing of mass spectrometric data. *Journal of Analytical Atomic Spectrometry* **26**, 2508–18. doi: 10.1039/C1JA10172B.

Paul B, Paton C, Norris A, Woodhead J, Hellstrom J, Hergt J and Greig A (2012) CellSpace: a module for creating spatially registered laser ablation images within the Iolite freeware environment. *Journal of Analytical Atomic Spectrometry* **27**, 700–6. doi: 10.1039/C2JA10383D.

Pereira MF, Castro A, Chichorro M, Fernández C, Díaz-Alvarado J, Martí J and Rodríguez C (2014) Chronological link between deep-seated processes in magma chambers and eruptions: Permo-Carboniferous magmatism in the core of Pangaea (Southern Pyrenees). *Gondwana Research* **25**, 290–308. doi: 10.1016/j.gr.2013.03.009.

Pesquera A and Pons J (1990) Le pluton hercynien de Aya (Pyrénées basques espagnoles). Structure, mise en place et incidences tectoniques regionals. *Bulletin de la Société Géologique, France* **8**, 13–21.

Porquet M, Pueyo E, Román-Berdiel T, Longares LA, Cuevas J, Ramajo J and the Geokin3DPyr (2017) Anisotropy of magnetic susceptibility of the Pyrenean granites. *Journal of Maps* **13**, 438–48. doi: 10.1080/17445647.2017.1302364.

Ríos LM, Galera JM, Barettino D and Hernán FJ (2002) *Mapa geológico de España, 1/50.000, Hoja nº 180, Benasque*. Madrid: Instituto Geológico y Minero de España.

Ríos LM, Lanaja JM, Rios JM and Marín FJ (1982) *Mapa geológico de España, 1/50.000, Hoja nº 179, Bielsa*. Madrid: Instituto Geológico y Minero de España.

Rodríguez-Méndez L, Cuevas J, Esteban JJ, Tubía JM, Sergeev S and Larionov A (2014) Age of the magmatism related to the inverted Stephanian-Permian basin of Sallent area (Pyrenees). In *Deformation Structures and Processes within the Continental Crust* (eds S Llana-Fúnez, A Marcos and F Bastida), pp. 101–11. Geological Society of London, Special Publication no. 394. doi: 10.1144/SP394.2.

Román-Berdiel T, Casas A, Oliva-Urcia B, Pueyo EL, Liesa C and Soto R (2006) The Variscan Millares granite (central Pyrenees): pluton emplacement in a T fracture of a dextral shear zone. *Geodinamica Acta* **19**, 197–211. 10.3166/ga.19.197-211.

Román-Berdiel T, Casas A, Oliva-Urcia B, Pueyo EL and Rillo C (2004) The main Variscan deformation event in the Pyrenees: new data from the structural study of the Bielsa granite. *Journal of Structural Geology* **26**, 659–77. doi: 10.1016/j.jsg.2003.09.001.

Schmidt MW (1992) Amphibole composition in tonalite as a function of pressure: an experimental calibration of Al-in-hornblende barometer. *Contributions to Mineralogy and Petrology* **110**, 304–10. doi: 10.1007/BF00310745.

Steiger RH and Jäger E (1977) Subcommission on Geochronology: Convention on the Use of Decay Constants in Geo- and Cosmochronology. *Earth and Planetary Science Letters* **36**, 359–62. doi: 10.1016/0012-821X(77)90060-7.

Tera F and Wasserburg G (1972) U-Th-Pb systematics in three Apollo 14 basalts and the problem of initial Pb in lunar rocks. *Earth and Planetary Science Letters* **14**, 281–304. doi: 10.1016/0012-821X(72)90128-8.

Ternet Y, Majesté-Menjoulas C, Canérot J, Baudin T, Cocherie A, Guerrot C and Rossi P (2004) *Notice Explicative, Carte géologique de la France (1/50000), feuille Laruns-Somport (1069)*. Orléans: BRGM.

Vissers RLM (1992) Variscan extension in the Pyrenees. *Tectonics* **6**, 1369–84. doi: 10.1029/92TC00823.